



NUMERICAL ESTIMATES OF THE RATE OF CONVERGENCE
FOR THE VORTEX SHEET METHOD

88-3796-CP

Elbridge Gerry Puckett[†]
Lawrence Livermore National Laboratory
Livermore, California 94550

ABSTRACT

We demonstrate numerically that the vortex sheet method for approximating solutions of the Prandtl equations converges to the exact solution when it is used to model Blasius flow. This is a random walk method and therefore the error is a random variable. We estimate the expected value and the standard deviation of the error as a function of the computational parameters. This allows us to estimate the dependence of the error on each parameter and hence to find the relation between the parameters which maximizes accuracy and efficiency. We also demonstrate that the proper choice of parameters leads to a reduced statistical error, thus allowing one to nearly achieve the expected rate of convergence without averaging the solution.

§1 INTRODUCTION

An important and difficult problem in computational fluid mechanics today is that of computing flows at large Reynolds numbers. Many methods which perform well at small Reynolds numbers suffer from numerical diffusion. Thus, in order to maintain a given level of accuracy, one must continually refine the computational parameters as the Reynolds number is increased. This leads to an increasingly expensive computation, eventually exceeding the limit of one's computational resources.

In 1972 Chorin [7] introduced the random vortex method in an effort to remedy this problem. The random vortex method is a grid-free particle method for approximating solutions of the Navier-Stokes equations. The particles, called 'vortices', carry concentrations of vorticity and the velocity field is determined from the vortex strengths and positions via the Biot-Savart law. The vortices are transported in this velocity field and then undergo a random walk in order to model the effects of diffusion. Subsequent investigation [12, 16, 18] has shown that for smooth initial data and in the absence of boundaries the error is independent of the Reynolds number, R . In fact, since the variance of the random walk decreases like \sqrt{R}^{-1} , the error in approximating the viscous term of the Navier-Stokes equations actually decreases with increasing R .

In his original paper [7] Chorin satisfied the no-slip boundary condition by creating vortices on the boundary. This algorithm has proven to be unsatisfactory since it tends to create an unreasonably large number of vortices, thereby resulting in an

overly expensive computation. In 1978 Chorin [8] introduced the vortex sheet method as an alternative means of satisfying the no-slip boundary condition. This is a numerical method for approximating solutions of the Prandtl equations. It also is a grid-free particle method in which the particles, called 'sheets', carry concentrations of vorticity. The velocity is uniquely determined from the sheet positions and their strengths. The sheets are advected in this velocity field and then undergo a random walk perpendicular to the boundary to approximate the viscous term of the Prandtl equations. During this random walk sheets are created at the boundary to (approximately) cancel the tangential velocity at the boundary.

The vortex sheet method may be used with the random vortex method to obtain a hybrid method for solving the Navier-Stokes equations in domains with solid boundaries. This is accomplished by using the vortex sheet method in regions close to the boundaries, referred to as the 'sheet layer', and using the random vortex method outside the sheet layer. The two methods are coupled by letting sheets which exit the sheet layer become vortices with the same circulation, letting blobs which enter the sheet layer become sheets with the same circulation, and letting the tangential velocity induced on the boundary by the random vortex method be the 'velocity at infinity' imposed on the Prandtl equations. Hybrid vortex methods of this type have been successfully used to model such problems as flow past a circular cylinder [4, 5, 25], driven cavity flow [6], boundary layer instability [9], flow past a backwards-facing step [23], turbulent combustion [11, 21, 22], and wind flow over a building [24]. For a more detailed description of this hybrid vortex method see [9] or [21].

Much work has been devoted to understanding the accuracy of the the vortex method, (i.e. the random vortex method without the random walk used to solve Euler's equations) [1, 2, 3, 10, 13, 14, 15]. Although less literature concerning the random vortex method is available there exist two convergence proofs [12, 16] and a numerical study of the convergence rate [18]. (All of this work is for the 2-d random vortex method in the absence of boundaries.) There is also a detailed numerical investigation of the convergence rate of a hybrid vortex method applied to flow past a rearward facing step [23].

In this paper we numerically demonstrate that the vortex sheet method converges when it is used to model Blasius flow. We estimate the expected value and standard deviation of the error for different combinations of the computational parameters. This allows us to estimate the dependence of the error on each parameter and hence to establish guidelines for choosing the parameters in a manner that optimizes accuracy and computational efficiency. We hope that this work will provide users of these hybrid methods with guidance in the task of selecting computational parameters for optimal accuracy and efficiency.

[†] This work was part of the author's PhD dissertation in the Mathematics Department at the University of California, Berkeley. Portions of this work were performed under the auspices of the Office of Naval Research under contract number N00014-76-C-0316 and the U. S. Department of Energy at the Lawrence Berkeley Laboratory under contract number DE-AC03-76SF00098 and the Lawrence Livermore National Laboratory under contract number W-7405-ENG-48.

Copyright © 1988 by the American Institute of Aeronautics and Astronautics, Inc. All rights reserved.

§2 THE METHOD

Let (x, y) denote coordinates which are parallel and perpendicular to the boundary respectively. Let (u, v) denote the corresponding velocity components, ω the vorticity, and ν the viscosity. Assume that the boundary is located at $y = 0$ and let $U_\infty(x, y)$ denote the 'velocity at infinity' which is imposed on the flow from outside the boundary layer. In vorticity formulation the Prandtl equations are

$$\omega_t + u \omega_x + v \omega_y = \nu \omega_{yy}, \quad (2.1a)$$

$$\omega = -u_y, \quad (2.1b)$$

$$u_x + v_y = 0, \quad (2.1c)$$

$$u(x, 0, t) = 0, \quad (2.1d)$$

$$v(x, 0, t) = 0, \quad (2.1e)$$

$$\lim_{y \rightarrow \infty} u(x, y, t) = U_\infty(x, t). \quad (2.1f)$$

In the vortex sheet method the vorticity at time $k\Delta t$ is approximated by a sum of linear concentrations of vorticity,

$$\tilde{\omega}^k(x, y) = \sum_{j=1}^N \omega_j b_h(x - x_j^k) \delta(y_j^k - y). \quad (2.2)$$

Each term of the sum in (2.2) is referred to as a vortex sheet. The j th sheet has center (x_j^k, y_j^k) and 'strength' or 'weight' ω_j . Here δ is the Dirac delta function, and $b_h = b(x/h)$ is the 'smoothing' or 'cutoff' function. The most commonly used cutoff is the 'hat' or 'tent' function originally proposed by Chorin [8],

$$b(x) = \begin{cases} 1 - |x| & |x| \leq 1, \\ 0 & \text{otherwise.} \end{cases} \quad (2.3)$$

The parameter h is often referred to as the 'sheet length' even though the support of b_h is typically of length nh for some integer $n > 1$. Since b_h has finite support and since $\delta(y_j - y)$ is 0 for $y \neq y_j$, we see that the j th sheet is simply a line segment parallel to the boundary which carries a delta function concentration of vorticity. For b_h defined by (2.3) each sheet has length $2h$ and the vorticity concentration varies linearly along the length of the sheet - having a value of ω_j at the center and 0 at the ends. We briefly discuss other possible choices for b_h at the end of this section.

We can use (2.1b) and (2.1f) to write the tangential velocity in terms of the vorticity,

$$u(x, y, t) = U_\infty(x, t) + \int_0^\infty \omega(x, s, t) ds. \quad (2.4)$$

Our approximation to u at time $k\Delta t$ is determined by (2.2) and (2.4),

$$\tilde{u}^k(x, y) = U_\infty(x, k\Delta t) + \sum_{j=1}^N \omega_j b_h(x - x_j^k) H(y_j^k - y), \quad (2.5)$$

where $H(y)$ is the Heaviside function,

$$H(y) = \begin{cases} 1 & y \geq 0, \\ 0 & \text{otherwise.} \end{cases}$$

From (2.5) we see that the jump in \tilde{u} along the j th sheet is $\omega_j b_h(x - x_j)$. This is the motivation for referring to the computational elements as 'vortex sheets'. To find the velocity

component normal to the boundary we first use (2.1c) and (2.1e) to write

$$v(x, y, t) = - \int_0^y u_x(x, s, t) ds. \quad (2.6)$$

Then, by approximating u_x with a centered divided difference, we obtain our approximation to v ,

$$\tilde{v}^k(x, y) = -\partial_x U_\infty(x, t) y \quad (2.7)$$

$$- \frac{1}{h} \sum_j \omega_j \left[b_h(x + \frac{h}{2} - x_j^k) - b_h(x - \frac{h}{2} - x_j^k) \right] \min(y, y_j^k).$$

Since \tilde{u}^k and \tilde{v}^k were constructed using (2.4) and (2.6) respectively the velocity field $(\tilde{u}^k, \tilde{v}^k)$ automatically satisfies equations (2.1b,c) and the boundary conditions (2.1e,f). Furthermore, given U_∞ , this velocity field is completely determined by the sheet positions (x_j^k, y_j^k) and their strengths ω_j .

The vortex sheet method is a fractional step method. The first step is the numerical solution of the convective part of equation (2.1a)

$$\omega_t + u \omega_x + v \omega_y = 0. \quad (2.8)$$

The second step is the numerical solution of the diffusive part of (2.1a)

$$\omega_t = \nu \omega_{yy} \quad (2.9)$$

subject to the no-slip boundary condition (2.1d). Given an approximation $(\tilde{u}^k, \tilde{v}^k)$ to the velocity field at k th time step the velocity at the next time step is determined as follows.

We first evaluate $(\tilde{u}^k, \tilde{v}^k)$ at the center of each sheet. Denote this velocity by $(\tilde{u}_j^k, \tilde{v}_j^k)$. Our numerical approximation to (2.8) is found by moving the center of each sheet one time step of length Δt in this direction to obtain,

$$(x_j^{k+1/2}, y_j^{k+1/2}) = (x_j^k, y_j^k) + \Delta t (\tilde{u}_j^k, \tilde{v}_j^k). \quad (2.10)$$

In order to approximate (2.9) subject to (2.1d) we first create sheets on the boundary. Let $a_i, i = 1, \dots, r$ denote equally spaced grid points at $y = 0$ with grid spacing h ; $a_{i+1} - a_i = h$. The sheet positions given by (2.10) in general induce a non-zero tangential velocity on the boundary, which we denote $\tilde{u}^{k+1/2}(x, 0)$. Let $u_i = \tilde{u}^{k+1/2}(a_i, 0)$ and let ω_{\max} denote a computational parameter called the 'maximum sheet strength'. Then for each i we create $q_i = \lceil |u_i| / \omega_{\max} \rceil$ sheets with centers $(a_i, 0)$ and strengths $-\text{sign}(u_i) \omega_{\max}$ where $\lceil x \rceil$ denotes the greatest integer less than or equal to x . The numerical solution of the diffusion equation (2.9) is found by letting all sheets, new and old, undergo a random walk in the y direction, reflecting those that go below the boundary. The new sheet positions at time $(k+1)\Delta t$ are therefore given by

$$(x_j^{k+1}, y_j^{k+1}) = (x_j^{k+1/2}, |y_j^{k+1/2} + \eta_j|)$$

where the η_j are independent, Gaussian distributed random numbers with mean 0 and variance $2\nu\Delta t$.

We wish to make several comments regarding the sheet creation algorithm here. First, note that in our presentation of the algorithm all sheets have magnitude ω_{\max} and that we create no sheets at a_i when $|u_i| \leq \omega_{\max}$. Hence, the no-slip boundary condition is satisfied at a_i only up to order ω_{\max} . Many workers (including Chorin [8, 9]) create sheets at the i th grid point whenever $|u_i| \geq \epsilon$ for some $\epsilon \ll \omega_{\max}$ such that $\omega_j \leq \omega_{\max}$ all j and the sum of the strengths of these sheets exactly cancel u_i . For example, ϵ might be chosen to be on the order of the computer's

round off error. However, since this algorithm creates more sheets than the one above, and since the work required to compute $(\bar{u}_j^k, \bar{v}_j^k)$ at the center of each sheet is, at best, $O(h N^2)$ where N is the number of sheets in the flow, this greatly increases the computational cost of the algorithm. Furthermore, numerical experiments to compare the two sheet creation algorithms [17] show no increase in accuracy when this latter, more costly sheet creation algorithm is used.

The second point we would like to make here concerns the manner in which the no-slip boundary condition is satisfied and its relation to the cutoff function b_h . As noted above, $\bar{u}^{k+1/2}(x, 0)$ is, in general, non-zero. Ideally one would like to add some function to $\bar{u}^{k+1/2}$ which can be represented by the sum of sheets, and which cancels $\bar{u}^{k+1/2}(x, 0)$ at all points x on the boundary but leaves $\bar{u}^{k+1/2}(x, y)$ unchanged for $y > 0$. In other words, we wish to find some function of the form $\sum \omega_i b_h(x - x_i) H(y_i - y)$ such that

$$\bar{u}^{k+1/2}(x, y) + \sum_i \omega_i b_h(x - x_i) H(y_i - y) = \begin{cases} \bar{u}^{k+1/2}(x, y) & y > 0, \\ 0 & y = 0. \end{cases}$$

In general this is not possible. However, one can find ω_i and (x_i, y_i) so that this holds exactly for $y > 0$ and within $O(h)$ for $y = 0$. For example, when b_h is defined by (2.3) choosing $x_i = a_i$ and $y_i = 0$ reduces the problem to that of finding the coefficients of a piecewise linear interpolant to $-\bar{u}^{k+1/2}(x, 0)$ with node points at the a_i (e.g. see [20]). In other words, we wish to find coefficients c_i such that

$$\sum_i c_i b_h(x - a_i) \approx -\bar{u}^{k+1/2}(x, 0).$$

In actual practice we approximate the left hand side of this expression by creating q_i sheets at a_i with strengths ω_{q_i} such that $|\sum \omega_{q_i} - c_i| \leq \omega_{\max}$.

This idea can be generalized to make use of higher order interpolation procedures. For example, one can replace b_h with the basis function for cubic splines (e.g. see [20]). In [17] we studied the effect such a b_h has on the accuracy and rate of convergence of the sheet method. However, in spite of the fact that the no-slip boundary condition is solved to higher order with this choice of b_h , extensive numerical experiments failed to reveal an improvement in the overall accuracy of the method. This situation is similar to that which occurs when one chooses the sheets so that the no-slip boundary condition is satisfied exactly at each a_i . For, although the no-slip boundary condition is being solved more accurately, other sources of error are not being reduced and, as a consequence, the overall error remains the same.

There are three computational parameters in the vortex sheet method, the time step Δt , the sheet length h , and the maximum sheet strength ω_{\max} . The only generally agreed upon constraint that these parameters must satisfy is the so called 'CFL' condition,

$$\Delta t U_{\max} \leq h \quad (2.11)$$

where $U_{\max} = \max U_{\infty}$. The justification usually given for (2.11) is that one wants to ensure that sheets move downstream at a rate of no more than one grid point per time step. This is an accuracy condition (as opposed to a stability condition) which ensures that information propagating in the streamwise direction will influence all features of the flow which are at least $O(h)$. We also propose another accuracy condition:

$$\omega_{\max} \leq C_0 h^2 / \Delta t \quad (2.12)$$

where C_0 is a constant with dimensions $1/L$ and L is a typical length scale. (Usually L is the length of the boundary.) This condition is a consequence of requiring that the degree with which we refine u as a function of y be of the same order as the degree with which we refine features in the streamwise direction, $O(U_{\max} / \omega_{\max}) = O(L/h)$, and then using (2.11). Note that since

$$\partial_x \omega_j b_h(x - x_j) = O(\omega_{\max}/h),$$

sheets induce local (non-physical) streamwise gradients in \bar{u} which are $O(\omega_{\max}/h)$. Condition (2.12) relates the size of these gradients to the time step. In §3 below we present numerical results which demonstrate the importance of (2.12).

§3 CONVERGENCE TO BLASIUS FLOW

Recall that Blasius flow [19] is a stationary solution to the Prandtl equations for flow past a semi-infinite flat plate $\{(x, y) : 0 \leq x < \infty, y = 0\}$ with a constant free-stream velocity that we take to be $U_{\infty} = 1$. It is a similarity solution which may be written in the form

$$u(x, y) = f'(\eta), \quad (3.1)$$

where

$$\eta = y / \sqrt{vx} \quad (3.2)$$

is the similarity variable and f satisfies the ordinary differential equation

$$ff'' + 2f''' = 0,$$

$$f(0) = 0, \quad f'(0) = 0, \quad \text{and} \quad f'(\infty) = 1.$$

We compute over a finite portion of the plate $\{(x, y) : 3h \leq x < 1 + 3h, 0 \leq y < \infty\}$. Whenever a sheet moves beyond the end of the plate we rescale its y coordinate according to (3.2) and place it at the other end of the plate, i.e. periodic boundary conditions at $x = 3h, 1 + 3h$ with appropriately scaled y coordinate. Thus, here we can take our typical length scale to be $L = 1$. Initially there are no sheets so that

$$u(x, y, 0) = \begin{cases} 1 & y > 0, \\ 0 & y = 0. \end{cases}$$

We compute until time $t = 2$ and measure the error between the exact solution (3.1) and the computed solution. Note that we report errors at one instant in time rather than averaging the computed solution over several time steps as in [8] and [23]. All runs reported here are with $\nu = 10^{-4}$ and with the cutoff (2.3). We measure the L^1 error in similarity coordinates $(x, \eta) = (x, y/\sqrt{vx})$ so that

$$\|u(\cdot, t) - \bar{u}(\cdot, t)\|_{L^1} = \int_{3h}^{1+3h} \int_0^{\infty} |u(x, \eta, t) - \bar{u}(x, \eta, t)| d\eta dx.$$

This has the effect of making our measurement of the error independent the viscosity ν . Otherwise, the L^1 error goes to zero like $\sqrt{\nu}$. In addition, we normalize the L^1 error by dividing this integral by

$$\|1 - u\|_{L^1} \approx 1.7208.$$

To begin we estimate the expected value of the L^1 error at time $t = 2$ by averaging the error over several trials, each trial having been run with a different random number sequence. We examine the error for a variety of $(\Delta t, h, \omega_{\max})$. In our work we have found that fixing h and ω_{\max} and letting $\Delta t \rightarrow 0$ results in little or no change in the error. This indicates that the errors due to temporal discretization are much smaller than other sources of error. This may be because we are computing a stationary flow. In what follows we only report results for which $\Delta t = h / U_{\max}$.

Table 1 contains our estimates of the expected value of the L^1 error for $40^{-1} \leq h \leq 5^{-1}$ and $640^{-1} \leq \omega_{\max} \leq 5^{-1}$. Each parameter decreases by a factor of 2 as one moves down a row or a column. Unless indicated otherwise the estimates in Table 1 are for averages over 25 trials.

First note that fixing h and Δt and decreasing ω_{\max} eventually results in a fixed level of error. Since Δt and h are constant it follows that the error which is decreasing depends on ω_{\max} alone. The 'plateau' at the bottom of the column is due to those sources of error which depend on Δt and h . For $h = 0.025$ the rate of decrease prior to reaching this plateau is roughly $O(\sqrt{\omega_{\max}})$. On the other hand, fixing ω_{\max} and decreasing h and Δt eventually leads to an increase in the error. If we agree to let $C_0 = 1/2L$ then this increase begins to occur when (2.12) is violated.

In Fig. 1 we plot the log of the errors in Table 1 versus $\log h^{-1}$ for various relationships between ω_{\max} and h . The first data point in each sequence is $h = 5^{-1}$ and $\omega_{\max} = 10^{-1}$. (For h fixed the abscissa corresponds to $\omega_{\max} = 10^{-1}, \dots, 80^{-1}$.) When $\omega_{\max} = O(h^2)$ the resulting curve is nearly linear. This indicates that the error due to ω_{\max} is sufficiently small that we can observe a dependence of the form $error = O(h^q)$. The slope of this line is $-0.7510 \approx -3/4$ implying $q \approx 3/4$. However, if instead we choose the data from the last row of Table 1 (the error due to ω_{\max} should be very small here), then we find $q \approx 2/3$. There is not enough data here to determine q beyond all doubt.

Table 2 contains the standard deviations of the errors in Table 1. In Fig. 2 we plot those standard deviations which correspond to Fig. 1. The nearly linear decay for $\omega_{\max} = O(h^2)$ corroborates our conclusion that when $\omega_{\max} = O(h^2)$ the error due to ω_{\max} is decreasing at least as rapidly as that due to h .

We made a sequence of runs under the assumption that the error is $O(\sqrt{\omega_{\max}}) + O(h^{2/3})$. We set $h = O(\omega_{\max}^{3/4})$, $\Delta t = h / U_{\max}$, and, starting with $\omega_{\max} = 40^{-1}$ and $h = 5^{-1}$, made five runs decreasing ω_{\max} by 2 each run. The results appear in Table 3. Note that the errors here are the results after only one trial, rather than being an estimate of the expected value of the error. We also report the L^2 error, the average error in the displacement thickness above the grid points (δ_{1av}), and the average error in the momentum thickness above the grid points (δ_{2av}). These latter two quantities were computed in physical coordinates and hence are $O(\sqrt{v}) = O(10^{-2})$. In Fig. 3 we compare the L^1 error from Table 3 with the conjectured rate of convergence. It is apparent that for this choice of parameters the error after only one trial decreases at a rate close to the anticipated one. Our experience with $q > 2/3$ has not produced results which are as consistently good as those shown here, but we still do not have enough evidence to unequivocally state that the optimal choice of q is $2/3$.

We have presented numerical evidence that the vortex sheet method converges to the exact solution when it is used to approximate Blasius flow. For this problem there is no noticeable dependence of the error on the time step as long as (2.11) is satisfied. However, there is a marked increase in the error when (2.12) is violated with $C_0 = 1/2L$. In particular, this occurs when ω_{\max} is fixed and $\Delta t, h \rightarrow 0$.

Based on our experiences computing Blasius flow we recommend choosing $\Delta t = h / U_{\max}$ and $\omega_{\max} \leq C_0 h^2 / \Delta t$ for some small $C_0 = O(1/L)$, and refining the parameters so that $\omega_{\max} = O(h^{2q})$ for some $2/3 \leq q \leq 1$. We have obtained good results with $q = 2/3$, without averaging the solution in any manner. We have demonstrated the effectiveness of this choice of parameters with a sequence of runs for which the instantaneous, unaveraged error is very close to the conjectured rate of convergence.

We conclude with a brief comparison between the results reported here and those in [23]. In the latter work the authors made measurements of the mean and variance of the L^2 error taken over a sequence of time steps rather than over independent trials. For laminar flow many of the conclusions they reach agree with ours here, in spite of the differences in the way the error was measured. In particular they found that both the mean and standard deviation of the error decrease roughly like $O(\sqrt{C})$, where C (for circulation) equals our $\omega_{\max} h$. For fixed h this agrees with our observation that the error is $O(\sqrt{\omega_{\max}})$.

Acknowledgements

The author would like to thank Alexandre Chorin and Ole Hald for their helpful comments and suggestions. He would also like to acknowledge fruitful discussions with Phil Colella, Maciej Pindera, and Jamie Sethian.

References

1. C. R. Anderson and C. A. Greengard, "On Vortex Methods," *Siam J. Numer. Anal.*, vol. 22, 1985.
2. J. T. Beale and A. Majda, "Vortex Methods I: Convergence in Three Dimensions," *Math Comp*, vol. 39, pp. 1-27, 1982.
3. J. T. Beale and A. Majda, "Vortex Methods II: Higher Order Accuracy in Two and Three Dimensions," *Math Comp*, vol. 39, pp. 29-52, 1982.
4. A. Y. Cheer, "A Study of Incompressible 2-D Vortex Flow Past a Circular Cylinder," *SIAM J. Sci. Stat. Comput.*, vol. 4, pp. 685-705, 1983.
5. A. Y. Cheer, "Unsteady Separated Wake Behind an Impulsively Started Cylinder in Slightly Viscous Fluid," *manuscript*, U. C. Davis, 1986.
6. Y. Choi, J. A. C. Humphrey, and F. S. Sherman, "Random Vortex Simulation of Transient Wall-Driven Flow in a Rectangular Enclosure," *submitted to JCP*, UC Berkeley ME Dept, 1986.
7. A. J. Chorin, "Numerical Study of Slightly Viscous Flow," *J. Fluid Mech.*, vol. 57, pp. 785-796, 1973.
8. A. J. Chorin, "Vortex Sheet Approximation of Boundary Layers," *J. Comp. Phys.*, vol. 27, pp. 428-442, 1978.

9. A. J. Chorin, "Vortex Models and Boundary Layer Instability," *SIAM J. Sci. Stat. Comput.*, vol. 1, pp. 1-21, 1980.
10. G. H. Cottet, *Convergence of a Vortex in Cell Method for the Two Dimensional Euler Equations*, Rapport Interne No: 108, Centre de Mathematiques Appliquees, Ecole Polytechnique, Paris, 1984.
11. A. F. Ghoniem, A. J. Chorin, and A. K. Oppenheim, "Numerical Modeling of Turbulent Flow in a Combustion Tunnel," *Philos. Trans. Roy. Soc. London*, vol. A304, pp. 303-325, 1982.
12. J. Goodman, "Convergence of the Random Vortex Method in Two Dimensions," *Comm Pure and Applied Math*, to appear.
13. C. A. Greengard, "Three Dimensional Vortex Methods," *Ph.D. Thesis*, U. C. Berkeley, 1984.
14. O. H. Hald and V. M. Del Prete, "Convergence of Vortex Methods for Euler's Equations," *Math Comp*, vol. 32, pp. 791-809, 1978.
15. O. H. Hald, "The Convergence of Vortex Methods, II," *Siam J. Num. Anal.*, vol. 16, pp. 726-755, 1979.
16. D. G. Long, "Convergence of the Random Vortex Method in One and Two Dimensions," *Ph.D. Thesis*, U. C. Berkeley, 1986.
17. E. G. Puckett, "A Study of the Vortex Sheet Method and Its Rate of Convergence," *Lawrence Berkeley Laboratory Preprint 23341*, 1987.
18. S. G. Roberts, "Accuracy of the Random Vortex Method for a Problem with Non-Smooth Initial Conditions," *J. Comp. Phys.*, vol. 58, pp. 29-43, 1985.
19. H. Schlichting, *Boundary-Layer Theory*, McGraw-Hill, New York, 1968.
20. M. H. Schultz, *Spline Analysis*, Prentice-Hall, Inc., Englewood Cliffs, N.J., 1973.
21. J. A. Sethian, "Turbulent Combustion in Open and Closed Vessels," *J. Comp. Phys.*, vol. 55, pp. 425-456, 1984.
22. J. A. Sethian, "Vortex Methods and Turbulent Combustion," in *Lectures in Applied Mathematics*, vol. 22, Springer Verlag, New York, 1985.
23. J. A. Sethian and A. F. Ghoniem, "Validation Study of Vortex Methods," *J. Comp. Phys.*, vol. 74, pp. 283-317, 1988.
24. D. M. Summers, T. Hanson, and C. B. Wilson, "A Random Vortex Simulation of Wind-Flow Over a Building," *Int. J. for Num. Meth. in Fluids*, vol. 5, pp. 849-871, 1985.
25. E. Tiemroth, "The Simulation of the Viscous Flow Around a Cylinder by the Random Vortex Method," *Ph. D. Thesis*, U. C. Berkeley Naval Arch. Dept, 1986.

Error in the L¹ Norm Averaged over 25 Trials

ω_{max}	$h \quad (\Delta t = h / U_{max})$			
	0.2	0.1	0.05	0.025
5^{-1}	0.4002	0.4538	0.5029	0.6755
10^{-1}	0.2989	0.2983	0.3290	0.4060
20^{-1}	0.2580	0.2239	0.2230	0.2891
40^{-1}	0.2663	0.1773	0.1657	0.1903
80^{-1}	0.2483	0.1636	0.1267	0.1346
160^{-1}	0.2529	0.1594	0.1088	0.0990
320^{-1}	0.2473	0.1528	0.1007	0.0778 [†]
640^{-1}	0.2511	0.1534	0.0857 [†]	0.0627 [‡]

Table 1 † = 5 trials, ‡ = 2 trials

Standard Deviation of the Errors in Table 1

ω_{max}	$h \quad (\Delta t = h / U_{max})$			
	0.2	0.1	0.05	0.025
5^{-1}	0.0734	0.0649	0.0519	0.0511
10^{-1}	0.0638	0.0521	0.0350	0.0373
20^{-1}	0.0475	0.0399	0.0279	0.0175
40^{-1}	0.0473	0.0239	0.0112	0.0165
80^{-1}	0.0243	0.0202	0.0126	0.0101
160^{-1}	0.0252	0.0104	0.0103	0.0075
320^{-1}	0.0146	0.0093	0.0069	0.0077 [†]
640^{-1}	0.0088	0.0068	0.0078 [†]	0.0060 [‡]

Table 2 † = 5 trials, ‡ = 2 trials

A Convergence Study with $h = O(\omega_{max}^{3/4})$ and $\Delta t = h / U_{max}$

ω_{max}	One Trial Per Row			
	L^1 norm	L^2 norm	$\delta_{1,av}$	$\delta_{2,av}$
40^{-1}	0.2817	0.2489	0.0044	0.00161
80^{-1}	0.1617	0.1756	0.0024	0.00070
160^{-1}	0.1044	0.1070	0.0013	0.00037
320^{-1}	0.0823	0.0915	0.0009	0.00029
640^{-1}	0.0592	0.0631	0.0007	0.00019

Table 3

Fig. 1 Log Error versus Log 1/h

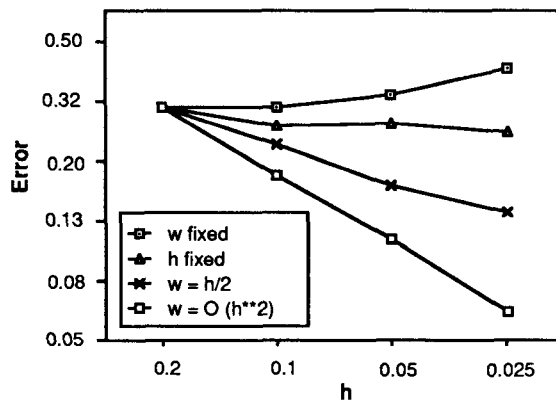


Fig. 2 Log Std Dev versus Log 1/h

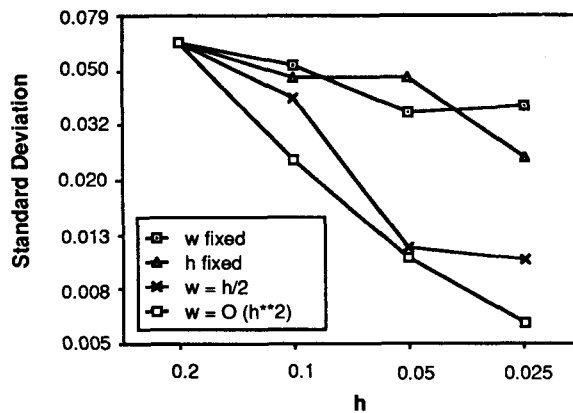


Fig. 3 Actual versus Predicted Rate

